Estimation of Needle Tip Location Using Ultrasound Image Processing and Hypoechoic Markers

Ian McSweeney, Brian Murphy and William M. D. Wright
School of Engineering – Electrical and Electronic Engineering
University College Cork
College Road, Cork, Ireland
Email: bill.wright@ucc.ie

***Abstract*—Ultrasound guidance is a common method used in procedures such as peripheral nerve blocks and biopsies. Accurate determination of the location of the needle tip is critical in many such procedures. Visual graduations on the needle may give an external estimate of the depth of the needle tip, but the tip itself may be difficult to find in the ultrasound image even with in-plane imaging. The needle tip echo may also be occluded by other hyperechoic regions in the image. The objective of the current work was to develop a simple technique to accurately estimate the location of the needle tip in an ultrasound image, using a set of hypoechoic reference markings on the shaft of the needle, with image processing to improve accuracy and minimize error. A unique set of discrete hypoechoic markings was made along the shaft of a 14-gauge (2.1 mm nominal outer diameter) needle to provide a number of needle location reference points in the ultrasound image. Ultrasound scans were obtained of the needle in agar-based tissue mimicking phantoms using an 8.0 MHz linear array. The resulting images were cropped and binarized using an intensity filter before morphological operations were applied to isolate the needle echo in the image. A straight line was fitted to the top edge of the needle echo and up to three adjacent reference markings were found along this line. These were then used to estimate the actual position of the tip in the image. The accuracy of the location was affected by the resolution of the ultrasound image and the probe frequency. Redundancy in the number of markings used increased the robustness of the technique.**

Keywords—Needle tip location, Needle marking, Image processing, US guidance

I. Introduction

Ultrasound (US) guidance is a common method of visualising the location of needles during percutaneous procedures such as peripheral nerve blocks [1]. During these procedures, the trajectory taken by the needle needs to be known with a high level of accuracy to avoid inadvertent damage to surrounding tissue, blood vessels or organs. The precise location of the needle tip should also be known as it is recommended that the epineurium is not penetrated with the needle to avoid any potential nerve damage [2].

One issue in US guidance is that very often the needle tip is difficult to locate precisely in the image. This may be due to poor contrast between the needle and the image background or the relative angle between the needle and the US beam [3]. A number of different techniques have been investigated for enhancing needle visibility during US imaging by image processing and modified needles [4, 5], to track needle motion during the procedure [6], and to track curved needles [7]. The tip location has also been inferred from external measurement of remaining needle length and entry angle, as was shown in [8]. Some techniques used adaptive beam steering to match the angle of the ultrasound beam with that of the needle to enhance visibility [9].

The purpose of the current study was to develop a simple technique for enhancing the needle visibility, using a combination of needle modification and image processing, whilst simultaneously allowing the location of the tip to be accurately inferred, even if the tip itself was not visible in the US image due to occlusion by another feature, or poor image contrast near the tip.

II. Method and Experiment

A unique set of hypoechoic markings was made on a needle to assist in its location in the US image. A number of different needle sizes and marking techniques were investigated. As an indicative example, three sections of a standard 14-gauge needle (with a nominal outside diameter of 2.1 mm) were removed to a depth of 0.2 mm by conventional milling, as shown in Fig. 1 to produce a series of discrete steps in the needle surface at different distances without unduly weakening the needle or exposing the central bore.

Fig. 1: Markings on a 14 gauge (2.1 mm nominal OD) needle.

This work was supported by Science Foundation Ireland (SFI) Research Frontiers Programme, grant no. 11/RFP.1/ECE/3119

Fig. 2: A typical agar-based tissue-mimicking phantom.

US images of the modified needle were acquired using an ESAOTE Pie Medical Falco 100 ultrasound scanning system using an 8.0 MHz L40 linear array and a Zarbeco USB frame grabber to transfer video and individual frames to a PC for storage and analysis using MATLAB®. A series of tissue-mimicking phantoms [10] was manufactured from a mixture of agar, de-ionized water and glycerol, using isopropanol to adjust the speed of sound in the phantoms to be approximately 1540 m/s. A typical test phantom was a flat rectangular block of approximately 120 x 50 x 30 mm, as shown in Fig. 2. A number of US images of the modified needle were acquired in agar phantoms at different angles and depths of insertion, with a typical image being shown in Fig. 3. The three milled surfaces in the top of the needle are clearly visible as discrete steps in the image. At 8.0 MHz, the wavelength is approximately 0.193 mm so that each step is of the order of a wavelength in height.

III. Image Pre-Processing

An algorithm was written in MATLAB® using the Image Processing toolbox to process the images as follows. The original image i was cropped to i_c remove on-screen menus and to isolate the region of interest (ROI). The cropped image i_c was then converted from RGB to a greyscale intensity g_c using the following weightings for the RGB luminance values:

$$g_c = (0.2989 * R) + (0.5870 * G) + (0.1140 * B). \quad (1)$$

A histogram of the cropped grayscale image g_c was then determined, with a typical example shown in Fig. 4. The highest grayscale levels correspond to the needle echo, yet the maximum frequency of occurrence corresponds to background detail that needs to be removed.

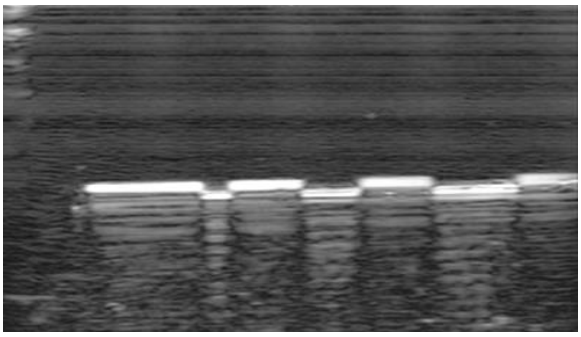

Fig. 3: Cropped grayscale image showing ROI.

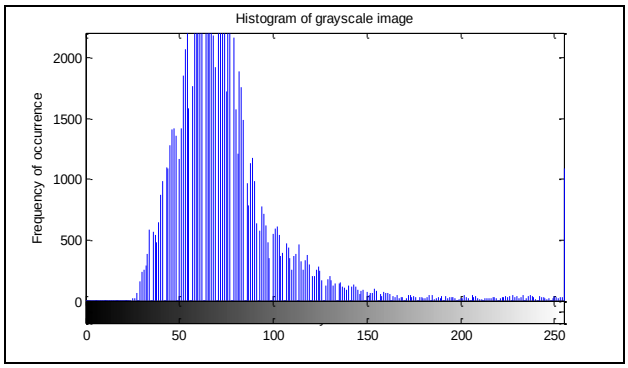

Fig. 4: Typical grayscale histogram.

A two-step segmentation process was then applied. First, the cropped grayscale image g_c was intensity filtered to f_c using a threshold level 120 grayscale levels below the maximum grayscale level detected in the image, which helped to normalize the threshold to the overall image contrast. This produced an image f_c with most of the background speckle removed, but blurred the feature edges and some undesirable regions remained in the image, primarily additional needle echoes or reverberations and other large high contrast regions. An extended-maxima transform was then applied with a 26-connected neighborhood to binarize the image to b_c whilst still preserving sufficient edge detail. The extended-maxima transform [11] is a useful method of combining regions of pixels with a constant intensity but with blurred region boundaries with pixel intensities below the threshold intensity, as it suppresses all maxima in the image with a grayscale less than the specified threshold.

This was followed by an area-opening morphological operation:

$$b_c \circ a = (b_c \ominus a) \oplus a, \quad (2)$$

which is simply an erosion of the binarized image b_c by the structural element a followed by a dilation of the result by a, with 8-pixel connectivity, to remove the remaining regions smaller than 200 pixels that were not likely to be part of the main needle echo. This resulted in an image m_c in which the needle echo was the predominant feature, with the hypoechoic markings still visible, as shown in Fig. 5. Note that one of the spurious needle reverberations still remains in the image.

Fig. 5: Processed and binarized image.

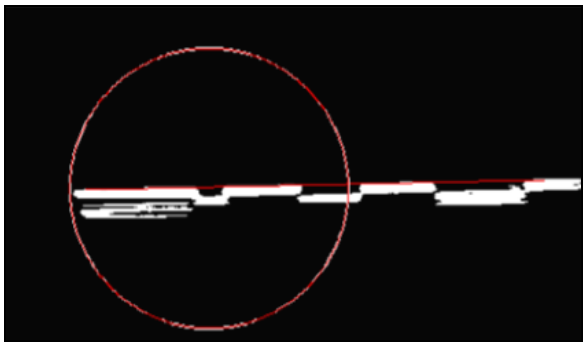

Fig. 6: Tip position estimate from a single needle marking.

IV. Marking Identification and Tip Location

Once the image had been successfully segmented and the needle echo region isolated, a straight line was fitted to the top surface (probe side) of the needle echo. Due to the thickness of the needle echo region, custom code was written to search within a pre-determined number of pixels of the left-most and right-most extremities of the needle region until the upper-most pixel at each end was identified. Additional code was then written to search one pixel below this top-surface line in the binarized image for groups of black pixels that would correspond to the hypoechoic grooves machined into the needle. Each continuous group of pixels so located was stored in an array. Due to noise in the original image, additional small hypoechoic regions could be misinterpreted as needle markings, and additional small hyperechoic regions could break up the desired echo from the larger needle markings into smaller sections, leading to false identification. Hence, another algorithm was written to assess whether adjacent markings should be ignored or combined together, as appropriate, using *a priori* knowledge of the size of the actual needle markings and their spacing. Each marking had a unique length allowing it to be identified separately. Hypoechoic regions along the line smaller than the minimum marking size would only be joined together if the distance between them was below a pre-determined proportion of the minimum distance between any two markings. Any hypoechoic region smaller than the smallest actual marking, and separated by a minimum distance from any adjacent marking was treated as noise and ignored.

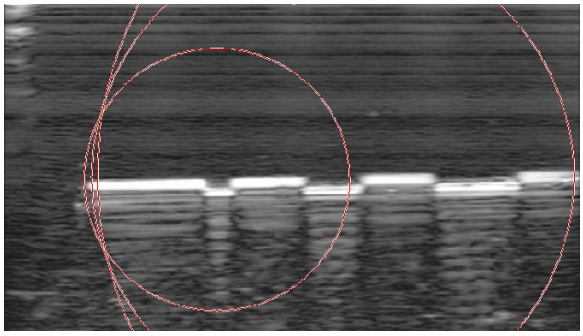

Fig. 7: Tip position estimates from three adjacent marks overlaid on the original cropped grayscale image.

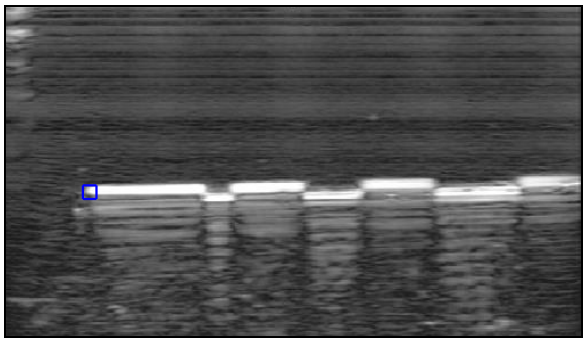

Fig. 8: Estimated tip location overlay showing margin of error.

Once a marking had been correctly identified, its geometric center in the image was found, from which a circle with a radius equal to the actual distance of the tip from the mark center was determined. The intersection of this circle with the top-surface line was found, as shown in Fig. 6. This gave a first estimate of the needle tip location from a single marking. The center of each marking detected in the image was used, as the position of this was least affected by the morphological operations used to segment the image, which tended to blur the steps at the edges of each marking.

V. Results

Fig. 7 shows the combined estimates of tip position from three adjacent needle markings, overlaid over the original cropped grayscale US image, g_c. Fig. 8 shows an overlaid bounding box that was drawn between the leftmost and rightmost intersections to indicate the tip position estimate and the margin of error, which was heavily influenced by the quality of the original US image, *i*. Fig. 9 shows the tip estimate where only two needle marks were visible in the image, which in this case shows a smaller difference between the tip position estimates. Fig. 10 shows a wider bounding box to indicate the increase in tip position estimate error when the original image quality is poor. Finally, Fig. 11 shows that the technique is still able to estimate the tip location from just the markings even when the tip itself is occluded in the original image by a spurious phantom echo.

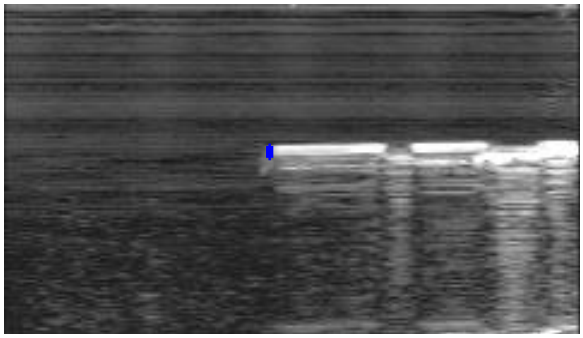

Fig. 9: Tip position estimate using two needle markings.

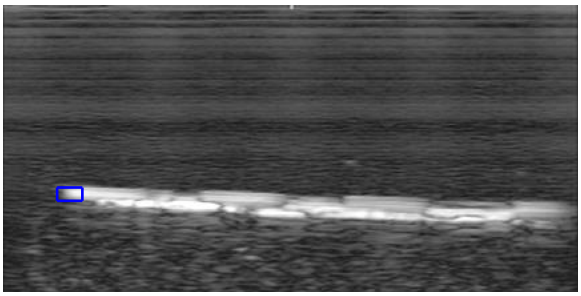

Fig. 10: Tip estimate with larger margin of error from a poor quality image.

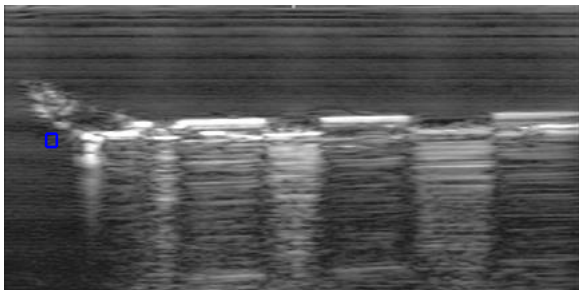

Fig. 11: Tip position estimate based on needle markings when tip is occluded in the image.

VI. Discussion

The technique was quite robust, with tip location estimates possible using only one or more markings, with a higher number of markings visible in the image providing a more reliable estimate. Hence the needle tip could be tracked as it was inserted, with the position estimate becoming more accurate as more of the needle markings became visible in the ROI. Needle insertion angles of between +15° and -15° from the horizontal in the image produced acceptable results, with larger angles reducing the clarity of the needle echo within the image, as expected. One of the primary limitations of the current work was the US scanner, which did not produce particularly good ultrasound images, especially when using smaller gauge needles. Hence, significant improvements would be expected with a higher resolution US scanning system.

VII. Conclusions and Future Work

A technique for estimating the position of a needle tip in US images has been successfully developed. Using a set of three discrete markings machined into the top surface of a 14-gauge needle allowed the markings to be isolated in the US image after image processing to binarize and segment the grayscale image using an intensity threshold filter, an extended-maxima transform and an area-closing algorithm. The known positions of the markings relative to the actual needle tip were used to estimate the tip location in the image, even when only one marking on the needle shaft was visible, or if the tip itself was not visible in the original image. Future work will investigate additional de-noising and segmentation methods, additional needle marking schemes and real time implementation.

Acknowledgments

The authors would like to thank Timothy Power and Michael O'Shea for their perseverance in needle marking, and Hilary Mansfield for repairing the scanner during the work.

References

[1] K.J. Chin, A. Perlas, V.W.S. Chan, and R. Brull, "Needle Visualization in Ultrasound-Guided Regional Anesthesia: Challenges and Solutions", Reg. Anesth. Pain Med., Vol. 33, Issue 6, pp. 532–544, 2008.

[2] A. Borgeat, "Regional Anesthesia, Intraneural Injection, and Nerve Injury: Beyond the Epineurium", Anesthesiology, Vol. 105, Issue 4, pp. 647-648, 2006.

[3] I. Schafhalter-Zoppoth, C. McCulloch and A. Gray, "Ultrasound visibility of needles used for regional nerve block: An in vitro study," Reg. Anesth. Pain Med., Vol. 29, Issue 5, pp. 480-488, 2004.

[4] D.I. Jandzinski, N. Carson, D. Davis, D.J. Rubens, S.L. Voci, and R.H. Gottlieb, "Treated Needles: Do They Facilitate Sonographically Guided Biopsies?", J. Ultrasound Med., Vol. 22, pp. 1233–1237, 2003.

[5] R.K. Deam, R. Kluger, M.J. Barrington and C.A. McCutcheon, "Investigation of a new echogenic needle for use with ultrasound peripheral nerve blocks", Anaesth. Intensive Care, Vol. 35, No. 4, pp. 582-586, 2007.

[6] J.-S. Hong, T. Dohi, M. Hasizume, K. Konishi and H. Nobuhiko, "A Motion Adaptable Needle Placement Instrument Based on Tumor Specific Ultrasonic Image Segmentation", Medical Image Computing and Computer-Assisted Intervention, Vol. 2488, pp. 122-129, 2002.

[7] S. H. Okazawa, R. Ebrahimi and J. Chuang, "Methods for segmenting curved needles in ultrasound images", Med. Image Anal., Vol. 10, Issue 3, pp. 330-342, 2006.

[8] N. Vaughan, V.N. Dubey, M.Y. Wee and R. Isaacs, "Real time length measurement of epidural tuohy needle during insertion", IET Sci. Meas. Technol., Vol. 7, Issue 4, pp. 215-222, 2013.

[9] S. Cheung and R. Rohling, "Enhancement of needle visibility in ultrasound-guided percutaneous procedures", Ultrasound Med. Biol., Vol. 30, Issue 5, pp. 617-24, 2004.

[10] E.L. Madsen, M. A. Hobson, H. Shi, T. Varghese and G.R. Frank, "Tissue-mimicking agar/gelatin materials for use in heterogeneous elastography phantoms", Phys. Med. Biol., Vol. 50, Issue 23, pp. 5597–5618, 2005.

[11] R. C. Gonzalez and R. E. Woods, Digital Image Processing, 2nd Edition. Prentice-Hall Inc., NJ, 2002.